

Technical Note: A 3-D rendering algorithm for electromechanical wave imaging of a beating heart

Pierre Nauleau and Lea Melki

Department of Biomedical Engineering, Columbia University, 1210 Amsterdam Avenue, New York, NY 10027, USA

Elaine Wan

Department of Medicine - Division of Cardiology, College of Physicians and Surgeons, Columbia University, 161 Fort Washington Avenue, New York, NY 10032, USA

Elisa Konofagou^{a)}

Department of Biomedical Engineering, Columbia University, 1210 Amsterdam Avenue, New York, NY 10027, USA
Department of Radiology, Columbia University, 622 W 168th Street, New York, NY 10032, USA

(Received 21 December 2016; revised 25 April 2017; accepted for publication 9 June 2017;
published xx xxxx xxxx)

Purpose: Arrhythmias can be treated by ablating the heart tissue in the regions of abnormal contraction. The current clinical standard provides electroanatomic 3-D maps to visualize the electrical activation and locate the arrhythmogenic sources. However, the procedure is time-consuming and invasive. Electromechanical wave imaging is an ultrasound-based noninvasive technique that can provide 2-D maps of the electromechanical activation of the heart. In order to fully visualize the complex 3-D pattern of activation, several 2-D views are acquired and processed separately. They are then manually registered with a 3-D rendering software to generate a pseudo-3-D map. However, this last step is operator-dependent and time-consuming.

Methods: This paper presents a method to generate a full 3-D map of the electromechanical activation using multiple 2-D images. Two canine models were considered to illustrate the method: one in normal sinus rhythm and one paced from the lateral region of the heart. Four standard echographic views of each canine heart were acquired. Electromechanical wave imaging was applied to generate four 2-D activation maps of the left ventricle. The radial positions and activation timings of the walls were automatically extracted from those maps. In each slice, from apex to base, these values were interpolated around the circumference to generate a full 3-D map.

Results: In both cases, a 3-D activation map and a cine-loop of the propagation of the electromechanical wave were automatically generated. The 3-D map showing the electromechanical activation timings overlaid on realistic anatomy assists with the visualization of the sources of earlier activation (which are potential arrhythmogenic sources). The earliest sources of activation corresponded to the expected ones: septum for the normal rhythm and lateral for the pacing case.

Conclusions: The proposed technique provides, automatically, a 3-D electromechanical activation map with a realistic anatomy. This represents a step towards a noninvasive tool to efficiently localize arrhythmias in 3-D. © 2017 American Association of Physicists in Medicine [<https://doi.org/10.1002/mp.12411>]

Key words: 3-D rendering, arrhythmia, electromechanical wave imaging, ultrasound

1. INTRODUCTION

Arrhythmia is a heart disease characterized by abnormal electrical activation of the heart wall. These diseases affect a large part of the population: for instance, the prevalence of atrial fibrillation was five million of people in the US in 2010.¹ These abnormal activation patterns can result in inefficient contraction of the cardiac muscle, resulting in poor blood delivery to the body and damage to vital organs. Clinically, the diagnosis of arrhythmias is based on the analysis of electrocardiograms (ECG). This method is noninvasive but, due to a low spatial resolution, it cannot accurately locate the source of arrhythmia.² Heart rhythm disorders can be treated by ablating the origin of abnormal activation. Invasive 3-D electroanatomical mapping systems are used by clinicians to

locate the arrhythmogenic source. This technique consists in probing the endocardial wall of the myocardium with a catheter to measure the electrical activity, while the location of the catheter is triangulated from an electrical or magnetic field.³ A 3-D shell of the heart depicting the electrical activation of the tissue is obtained. However, this mapping strategy is time-consuming (the procedure time can vary from 30 to 60 min depending on the pathology and the mapping system used⁴⁻⁶), operator-dependent, invasive and limited by accessibility of the tissue. Electromechanical wave imaging (EWI) is an ultrasound-based method that can noninvasively characterize the electromechanical activity of the heart, i.e., the time at which a point of the myocardium starts contracting after being electrically activated.⁷ EWI can be summarized in two steps: (a) the minute displacements and the incremental

strains of the myocardium are estimated using high-frame rate echographic acquisitions and RF-speckle-tracking techniques; (b) the temporal evolution of the strain is analyzed in each point of the myocardium to determine the electromechanical activation time.⁷ EWI has been shown capable of mapping the activation sequence of the myocardium in the four chambers of the heart of human and canine models in normal rhythm or paced,^{8–10} of locating pacing sites,¹¹ of characterizing and mapping focal arrhythmias.¹² The obtained maps have been recently validated against electroanatomical mapping in a large animal model.^{13,14} The electromechanical propagation in a beating heart being a complex 3-D phenomenon, EWI is usually applied to different standard echocardiographic views (e.g., four-chamber, two-chamber, and three-chamber apical views). The resulting 2-D maps are then imported in a 3-D visualization software and manually registered to create a pseudo-3-D view.¹⁴ This process is time-consuming, operator-dependent and the resulting pseudo-3-D map is not easy to interpret for clinicians.

The goal of the present technical note was to present an automated technique to generate full 3-D maps depicting the electromechanical activation based on EWI data acquired in four different echocardiographic views. The method is illustrated with two examples.

2. MATERIAL AND METHODS

2.A. Experimental protocol

This study complied with the Public Health Service Policy on Humane Care and Use of Laboratory Animals and was approved by the Institutional Animal Care and Use Committee of Columbia University. Two male adult mongrel canines (weight = 22 and 24.5 kg) were used in this study. They were anesthetized with an intravenous injection of propofol (2–5 mg kg⁻¹). During the procedure, the animals were positioned supine on a heating pad and mechanically ventilated with a rate- and volume-regulated ventilator on a mixture of oxygen and isoflurane (0.5–5%). The chest was opened by left lateral thoracotomy with electrocautery and the heart was exposed by removing a rib. The heart of one canine was imaged with ultrasound while in normal sinus rhythm. The heart of the second animal was imaged while externally paced: a bipolar electrode was sutured onto the epicardial wall, in the lateral area of the left ventricle; this electrode was connected to a data acquisition system (NI USB-6259, National Instruments, Austin, TX, USA), which sent a pacing signal (amplitude 10 v, pulse width 2 ms, cycle length 500 ms). For acoustic impedance matching purposes, the thoracic cavity was filled with saline during ultrasound acquisitions.

2.B. Ultrasound acquisition

The RF channel data were acquired using a 2.5 MHz center frequency phased array (P4-2 ATL/Philips, Andover, MA, USA) connected to a research echographic scanner (V-1 Verasonics, Kirkland, MA, USA). Diverging wave imaging was

used to achieve a frame rate of 2000 frames per second. Two-second acquisitions were recorded to ensure visualization for at least one cardiac cycle. This high frame rate acquisition was followed by an anatomical imaging sequence (standard 64-line B-mode with 30 fps). The ECG signal recorded synchronously with ultrasound data using an ECG unit (77804A, HP, Palo Alto, CA, USA) was used to temporally align the high frame rate data with the anatomical images.

Four different apical views were acquired for each canine. They were chosen to be easily obtained and reproduced by trained echocardiographers: three are standard echographic views and one additional custom-defined view completes the angular coverage. The first view is the “four-chamber” view: the probe is placed at the apex of the heart and rotated until the four chambers (two atria and two ventricles) are optimally visualized. This view serves as a reference: a counterclockwise rotation of 60° of the transducer yields the “two-chamber” view (left atrium and left ventricle), while a clockwise rotation enables visualization of the “three-chamber” view (left atrium and left ventricle, right ventricle).¹⁵ An extra view, called “3.5-chamber” view, is acquired between the “four-chamber” and the “two-chamber” planes. The orientations of these different views are depicted in Fig. 1.

2.C. Electromechanical wave imaging

The RF data were processed independently for each echocardiographic view with the previously developed and validated EWI technique (Fig. 2).^{7–14} A delay-and-sum algorithm was used to reconstruct the series of RF images from the signals received by the elements of the phased array.¹⁶ These beam-formed images present a field of view of 90° for 128 lines (i.e., an angular sampling of 0.7°). The axial sampling frequency was 20 MHz (i.e., an axial sampling of 0.0385 mm). Axial displacements were estimated between successive RF frames using a fast 1-D RF-based cross-correlation algorithm¹⁷ with a window length of 10λ (6.2 mm) and an overlap of 90%. The contour of the myocardium was manually segmented on the first frame of the anatomical imaging sequence. Subsequently, the estimated displacements were used to automatically track the contour throughout the cardiac cycle. Axial incremental strains in the myocardium were calculated between consecutive RF frames using a least-squares estimator with a 5 mm kernel.¹⁸ Strains characterize the mechanical behavior of the myocardium: positive strains reflect a lengthening while negative strains indicate a shortening of the tissue. The electromechanical activation of a point of the heart thus corresponds to a change of sign, i.e., a zero-crossing of the strain curve (positive-to-negative or negative-to-positive according to the orientation of the tissue).⁹ An isochrone map depicting the electromechanical activation in each point of the myocardium was generated by detecting the time of occurrence of the first zero-crossing after the onset of the electrical activation (beginning of the QRS). The zero-crossings were semi-automatically obtained in 60–100 randomly selected regions. Cubic interpolation was then used to generate a smooth continuous isochrone map. This process

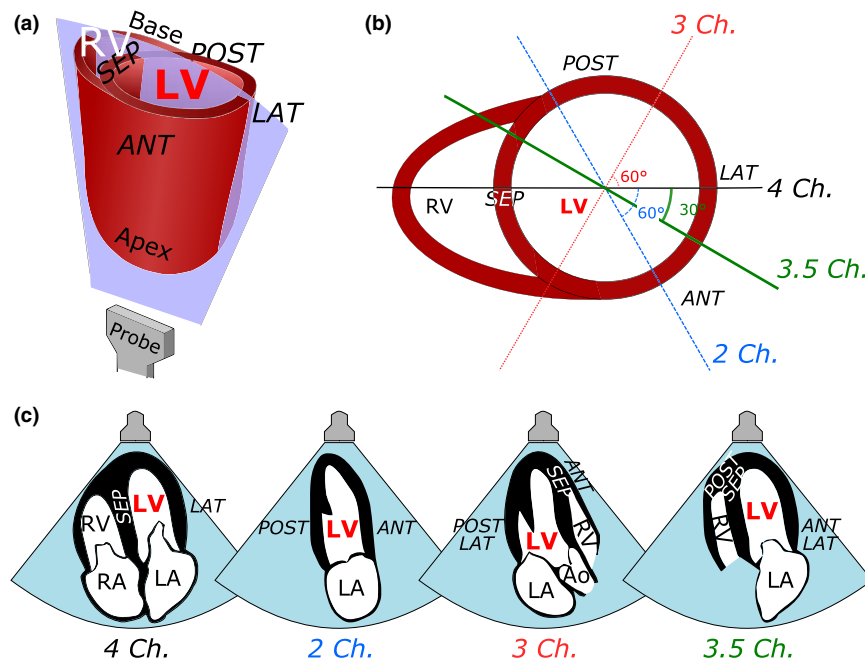


FIG. 1. (a) Ultrasonic acquisition of a four-chamber view (only the ventricles are represented here) of the heart. (b) View from the heart base of the relative positions of the four planes of imaging. (c) Schematic pictures of the heart chambers as seen in the four different echocardiographic views. RV/LV: right/left ventricle, RA/LA: right/left atrium, Ao: aorta, LAT: lateral, SEP: septum, ANT: anterior, POST: posterior.

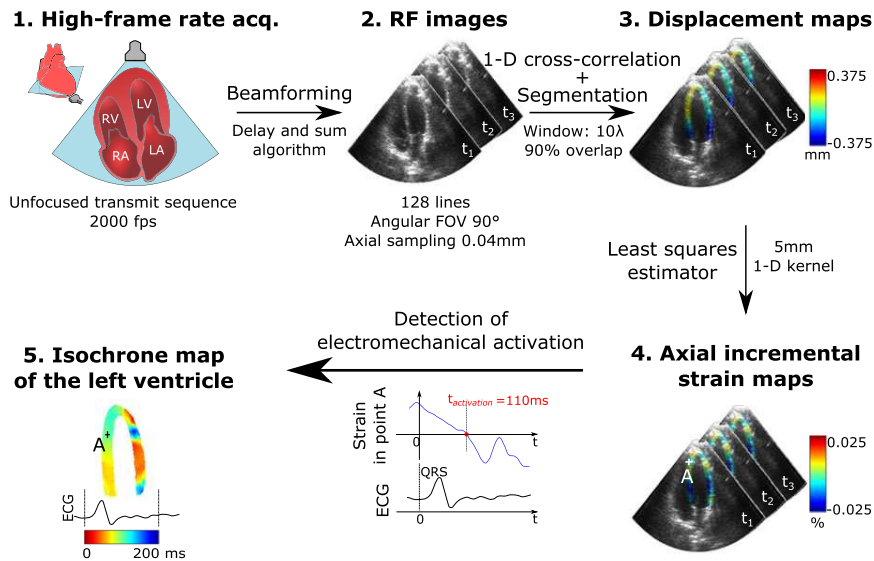


FIG. 2. EWI algorithm: 2-D images of the heart are acquired at a high-frame rate, the axial displacements, and the incremental strains of the myocardium are estimated; the zero-crossings of the strains indicating the electromechanical activation are detected for each point in order to generate an activation map.

was repeated for each of the four acquired views. Although this method can be applied to map the electromechanical activation in the four chambers of the heart,¹⁴ this study focused only on the left ventricle (LV).

2.D. Creation of a 3-D electromechanical activation map

The four isochrone maps served as an input to the customized algorithm built on Matlab (Matlab, The Mathworks,

Inc., Natick, MA, USA) we propose to generate a 3-D activation map. Two hypotheses were made to generate the 3-D map: (a) the different views are organized as in the theoretical case, Fig. 1; (b) the apical points and the median axes on the four different views are collocated and correspond to the apical point and the median axis of the 3-D matrix.

The algorithm started with the detection of the median axis of one of the 2-D views, referred to as z-axis. For each position along this z-axis, a search on the perpendicular axis was performed to detect the location (i.e., the radial distance

from the z -axis) and the activation time values of the points of the walls [Fig. 3(a)]. These activation time values were written in a 3-D matrix at a position defined by the polar coordinates: calculated radius, theoretical angle (depending on the considered view), and altitude z on the z -axis. The detection of the radius and activation time was repeated in the four different views for the same z -axis value. For a given z value, the 3-D matrix thus had eight series of values spread around a more or less circular section [Fig. 3(b)]. For each radial position, a linear interpolation between these eight different points yielded a smooth profile around the circumference [Fig. 3(c)]. These last steps were repeated for each z position, i.e., for each slice of the heart from the apex to the base, resulting in a 3-D matrix describing the geometry and the electromechanical activation times. The 3-D matrix was finally transformed from polar coordinates to cartesian coordinates. Using the same algorithm, the user can choose to visualize the full thickness of the myocardium or only the epicardial or endocardial shell. The location of the four initial echographic views was saved in a different 3-D matrix.

The resulting 3-D matrices were visualized in Amira 5.3.3 (Visage Imaging, Chelmsford, MA, USA) using commercial volume rendering algorithms. A standard physics colormap was used to visualize the 3-D maps. A monochromatic map and a thresholding method were used to generate a movie of the EW propagation.

For comparison purposes, the previously used pseudo-3-D views were constructed.¹⁴ The four 2-D activation maps

corresponding to the four echocardiographic acquisitions were manually coregistered in Amira 5.3.3 using anatomical landmarks (i.e., the position of the apex).

2.E. Comparison of the rendering methods

The proposed 3-D rendering method was compared against the manual coregistration method according to two criteria: the time of processing and the interoperator dependency. Two operators generated a 3-D and a pseudo-3-D view using the two datasets described in paragraph II. A 2-D correlation was used to quantify the similarity between the two independently generated 3-D views. Ultimately, these 3-D figures would be used by clinicians to locate areas of earliest or latest activation. Therefore, the difference between the estimated location of earliest (respectively latest) activation between the two independently generated 3-D views was also considered as an important index.

2.F. Impact of acquisition errors

Two kinds of errors can occur during acquisition: (a) the median axis of the different views may not be aligned due to a movement of the physician between the four successive acquisitions; and (b) the angular position of the acquisitions may be different from the ones assumed in the algorithm. The first case was studied by comparing the 3-D calculated volume with a second volume for which the median axes were rotated by 10° in each view. The second case was studied by

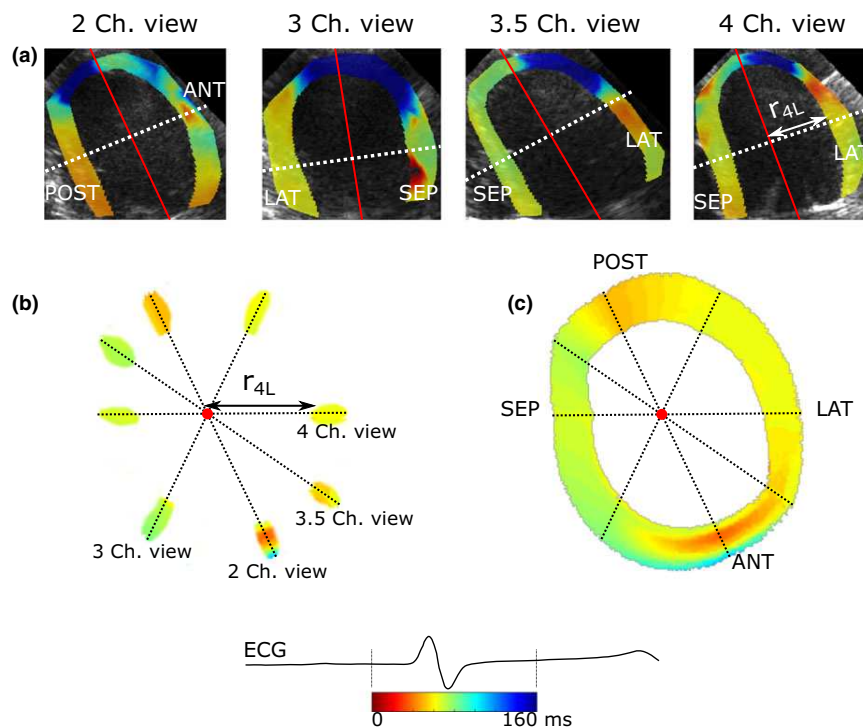


FIG. 3. (a) Isochrone maps generated from the four acquisitions for normal rhythm. The median axis is indicated with a solid line, while the dotted lines correspond to the considered transverse slice. (b) For the considered slice, in each view, the radial positions of the walls (e.g., r_{4L}) and the activation time values are extracted and organized in a 3-D matrix, in polar coordinates. (c) A linear interpolation around the circumference yields a smooth map.

comparing the 3-D calculated volume with a second volume, for which the values extracted in the 2-D slices had errors of 5° (i.e., the value normally placed at 0° for the 4-chamber view was placed at 5°). The respective values of 10 and 5° were chosen as reasonable errors: an error greater than those are likely to be noted on the B-mode image by the clinician, during the acquisition.

The indices used for the comparison of the two rendering methods (section 2.E.) were used to quantify the impact of these acquisition errors on the 3-D volume.

3. RESULTS

The proposed 3-D rendering method was applied to data acquired on a canine heart in normal sinus rhythm. The different steps of the algorithm are illustrated for one slice along the z-axis of this case, Fig. 3. The resulting shell is presented Fig. 4(b), alongside the pseudo-3-D view, Fig. 4(a). The same process was applied to the data acquired in a canine heart paced from the antero-lateral wall. The resulting 3-D matrix and the pseudo-3-D view are shown in Fig. 5. Snapshots of the movies of activation are depicted in Fig. 6 for normal sinus rhythm, (a), and paced rhythm, (b). For visualization purposes, the propagation is depicted on the epicardial shell rather than on the full myocardial matrix.

Table I presents a quantitative comparison of the two 3-D rendering methods in terms of calculation time and operator-dependency.

Table II indicates the errors resulting from a violation of the hypotheses during the acquisition: namely, a misalignment of the median axis or an angular position of the view differing from the conventional case (Fig. 1).

4. DISCUSSION

A method to visualize the electromechanical activation of the myocardium in 3-D in a chamber of the heart has been presented. The method was applied in two cases with

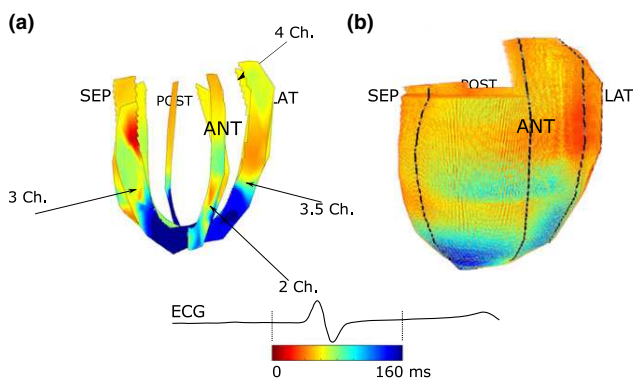


FIG. 4. (a) Pseudo-3-D view and (b) 3-D rendering of the activation map of the left ventricle of a canine in normal sinus rhythm. Black lines indicate the position of the imaging planes. The point of earliest activation is in the septal region. LAT: lateral, SEP: septum, ANT: anterior, POST: posterior.

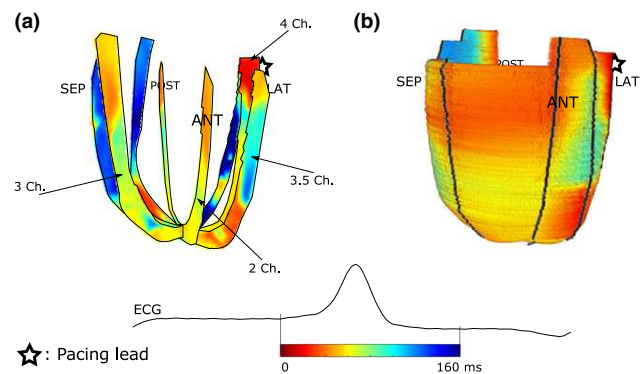


FIG. 5. (a) Pseudo-3-D view and (b) 3-D rendering of the activation map of the left ventricle of a canine while pacing from the lateral wall. Black lines indicate the position of the imaging planes. The point of earliest activation is in the lateral wall. LAT: lateral, SEP: septum, ANT: anterior, POST: posterior.

different activation patterns (a canine in normal sinus rhythm and a canine paced from the lateral wall) and was compared to our previous pseudo-3-D rendering technique. The proposed method is automated while the pseudo-3-D views are generated manually, which improves the time-efficiency of the new technique (7 min vs. \sim 29 min). The automation aspect also reduces the operator dependence: the 3-D volumes calculated by two different operators are highly similar and the important points are detected at positions separated by only a few millimeters (Table I). The reproducibility of the EWI technique itself (i.e., in 2-D) has been assessed in a separate study: the variation in activation times between two consecutive acquisition was found between 0.02 and 25.31%, with an average variation of 6.19%.¹⁹ Additionally, it is worth noting that the pseudo-3D map is merely an image, while the 3-D map is a 3-D set of data on which calculation can be performed. For instance, the average of the activation times through the lateral wall of the left ventricle can be calculated in 3-D and compared to the average of the activation times in the septal wall. Finally, the resulting 3-D shells provide structural information of clinical utility overlaid on a realistic anatomy. This representation is more user friendly, especially as it is modeled on what is already offered to clinicians by the existing electroanatomical systems (EnSite from St. Jude Medical, Secaucus, NJ, USA or CARTO from Biosense-Webster, Diamond Bar, CA, USA). This electromechanical activation shell is thus easier, for the clinician, to interpret than the pseudo-3-D map.

The electromechanical activation patterns depicted by the pseudo-3-D and the 3-D maps correspond to the expected electrical activation sequence for the two studied situations. For the normal sinus rhythm case, the electrical signals are generated spontaneously at the sinus node, in the right atrium. The signals travel through the atrium, the atrio-ventricular node, the bundle of His and finally through the ventricular myocardium, following the Purkinje fiber network. In the ventricle, the activation pattern is complex, originating from multiple locations depending on the fiber network. This

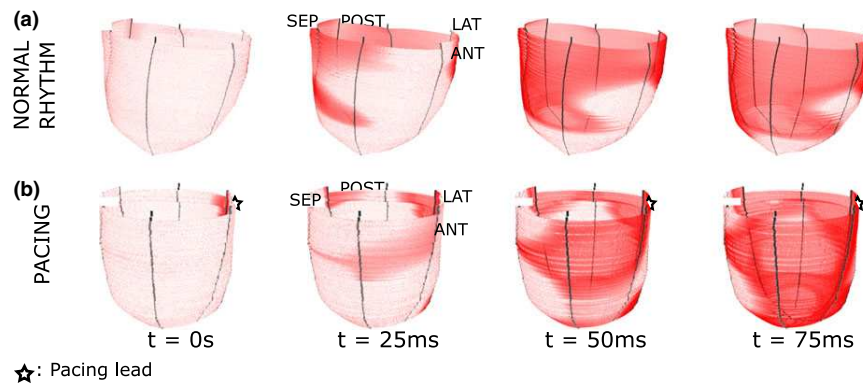


FIG. 6. Snapshots of the movie of the EW propagation in the left ventricles of a canine (a) in normal sinus rhythm and (b) pacing from the lateral wall. Black lines indicate the position of the four planes of imaging.

TABLE I. Quantitative comparison of the 3-D rendering methods.

	Normal		Paced	
	3-D	Pseudo-3-D	3-D	Pseudo-3-D
Time (mn)	8	30	5	28
Similarity (%)	87.3	27.6	93.2	28.0
ΔD_{Latest} (mm)	6.3	49.8	1.1	35.3
$\Delta D_{\text{Earliest}}$ (mm)	3.3	49.5	1.1	18.9

TABLE II. Estimation of the errors resulting from a mistake during the acquisition.

	Med. Ax. error		Ang. Pos. error	
	Normal	Paced	Normal	Paced
Similarity (%)	53.8	57.4	81.5	74.7
ΔD_{Latest} (mm)	7.1	2.9	1.2	1.7
$\Delta D_{\text{Earliest}}$ (mm)	3.3	3.4	1.8	1.7

theoretical description actually corresponds to the observations of the 3-D map (Fig. 4) and the movie [Fig. 6(a)]: (a) an earlier activation is noticed in the base-middle part of the ventricle, compared to the apex; (b) the point with the earliest activation is located in the septum; (c) multiple points located in different regions (septum, posterior, lateral) of the heart are activated at the same time. For the paced rhythm model, the activation pattern is simpler: the EW should originate from a single point, the pacing lead. In the case studied, the pacing lead was placed in the basal region of the lateral wall. The region of the earliest activation indeed coincided with the position of the lead [Figs. 5 and 6(b)].

The proposed 3-D rendering method represents a step towards a noninvasive, fully automated characterization of the electromechanical activation of the whole heart in real time. However, a few limits of the method should be acknowledged. First, the 3-D shell is generated by combining four

independent activation maps. The temporal registration of the maps is ensured by ECG-gating. The spatial registration, based on two hypotheses, may be less reliable. The ultrasound acquisitions are operator-dependent: the echocardiographic views are not always acquired with the angles defined conventionally and the median axes of the different views may not exactly coincide. The impact of these errors was studied (Table II) and the resulting error in the location of the earliest and latest activated points was found to be less than 7.1 mm. The size of the area ablated by the clinician to terminate an arrhythmia being of a few centimeters,²⁰ the proposed 3-D activation map should provide a sufficient accuracy. Second, the algorithm only used four views to generate a 3-D activation map. The angular sampling, between 30 and 45°, corresponds at the mid-level to a distance between 14 and 21 mm. This sampling is sufficient to detect global activation patterns (such as normal or paced rhythms) but small arrhythmogenic sources (such as the ones responsible for atrial fibrillation or flutter) might be difficult to accurately detect. Additional nonstandard views could be taken to increase the amount of information but a trade-off has to be found between accuracy, total duration of the acquisition, and reproducibility of the additional views. These two limits could be overcome, in the future, by using a 2-D probe to perform 3-D echographic acquisitions.

5. CONCLUSION

A 3-D rendering algorithm to generate electromechanical activation maps of the left ventricle of a beating heart was presented. This technique was applied to map the activation pattern under two conduction schemes in a large animal model: a normal sinus rhythm and a paced rhythm. The automatically generated 3-D maps depict in a clear way the propagation of the electromechanical wave. This methodology combined with the EWI technique may thus provide clinicians with an efficient noninvasive tool to characterize arrhythmias.

This 3-D rendering technique could also be applied for other types of 2-D functional maps that need to be mapped to the 3-D structure of the heart.